Concentration Gradient Effects of Sodium and Lithium Ions and Deuterium Isotope Effects on the Activities of H^+-ATP Synthase from Chloroplasts

M.-F. Chen, J.-D. Wang, and T.-M. Su*
Department of Chemistry, National Taiwan University, Taipei, Taiwan

ABSTRACT We explored the concentration gradient effects of the sodium and lithium ions and the deuterium isotope's effects on the activities of H^+-ATP synthase from chloroplasts (CF_0F_1). We found that the sodium concentration gradient can drive the ATP synthesis reaction of CF_0F_1. In contrast, the lithium ion can be an efficient enzyme-inhibitor by blocking the entrance channel of the ion translocation pathway in CF_0. In the presence of sodium or lithium ions and with the application of a membrane potential, unexpected enzyme behaviors of CF_0F_1 were evident. To account for these observations, we propose that both of the sodium and lithium ions could undergo localized hydrolysis reactions in the chemical environment of the ion channel of CF_0. The protons generated locally could proceed to complete the ion translocation process in the ATP synthesis reaction of CF_0F_1. Experimental and theoretical deuterium isotope effects of the localized hydrolysis on the activities of CF_0F_1, and the energetics of these related reactions, support this proposed mechanism. Our experimental observations could be understood in the framework of the well-established ion translocation models for the H^+-ATP synthase from *Escherichia coli,* and the Na^+-ATP synthase from *Propionigenium modestum* and *Ilyobacter tartaricus*.

INTRODUCTION

The enzyme activities and related reaction energetics of the membrane-bound ATP synthases (F_0F_1-ATPases) have received considerable attention since the 1960s, when Mitchell published his pioneer work on the chemiosmotic theory (1,2). Among the ATP synthases from various possible biological sources, the best-characterized and most intensively studied systems were the two homologs of H^+-ATP synthases from *Escherichia coli* (EF_0F_1) and the chloroplast of spinach (CF_0F_1) (3–7), and the Na^+-ATP synthases from *Propionigenium modestum* and *Ilyobacter tartaricus* (Na^+-F_0F_1) (8–11). It is generally accepted that in nature, the proton is the only energy carrier in the enzyme reactions of the former ATP synthase, whereas the sodium ion is the major energy carrier for the latter ATP synthase. Moreover, it was demonstrated that Na^+-ATP synthases could also translocate the protons and lithium ions (8–11). These enzymes can be driven by the chemical potentials originating from the concentration gradient and/or membrane potential. Apparently these homologous systems do not respond to these driving forces in the same way. Variations in activity behaviors were observed among these enzymes (3–11).

To understand the molecular mechanism of energy transduction through the proton or sodium ion translocation in ATP synthases, the EF_0 and Na^+-F_0 subunits were studied by Aksimentiev et al. (12) and Xing et al. (13), respectively. Armed with the available information on the protein structures involved, these two independent research groups used molecular dynamics calculations and/or mesoscopic stochastic methods to uncover the underlying molecular mechanism of torque generation in these two systems. These studies showed that the basic operating principle of EF_0 and Na^+-F_0 is essentially the same (13).

As mentioned above, the CF_0F_1 ATP synthase from chloroplasts was well-demonstrated to be driven by the translocation of protons. In contrast, the possible concentration gradient effects of sodium and lithium ions on enzyme activities have not been explored. Here we report that in the case of CF_0F_1, sodium ions can be used to drive the ATP synthesis reaction, whereas lithium ions can act as a blocker in the ATP synthesis reaction. In the course of this research, an additional ion translocation mechanism in the ATP synthesis reaction was evident, and was attributed to localized hydrolysis reactions of the lithium or sodium ion in the ion channel of CF_0. These observations were further supported by experiments on the deuterium isotope's effects on the enzyme activities of CF_0F_1, and by ab initio theoretical calculations regarding the energetics of the hydrolysis reactions. Based on correlations of the conserved homologous amino-acid sequences of CF_0 with those of EF_0 and Na^+-F_0, the unique activity behaviors of CF_0F_1 in the presence of sodium and lithium ions can be understood in the framework of the general molecular mechanisms of ion translocations developed for EF_0F_1 and Na^+-F_0F_1 (12,13).

Submitted July 20, 2008, and accepted for publication December 5, 2008.

*Correspondence: tmsu@rs350.ch.ntu.edu.tw

Editor: Robert Nakamoto.

0006-3495/09/03/2479/11 $2.00

doi: 10.1016/j.bpj.2008.12.3910

MATERIALS AND METHODS

Preparations of CF_0F_1, liposomes, and reconstituted proteoliposomes and measurements of initial ATP synthesis rates of CF_0F_1

The preparation of CF_0F_1 from the chloroplasts of spinach, and the reconstitution of proteoliposomes, followed general procedures developed by Gräber et al. (3–7,14) and Rigaud et al. (15). The liposomes consisted of phosphatidylcholine and phosphatidic acid, and were prepared by the well-established procedures of sonification and dialysis (4,5). The diameters of the final proteoliposomes were in the range of 100–110 nm. Because we measured the capabilities of proton, sodium, and lithium ions to drive the ATP synthesis reactions through CF_0F_1, different buffer solutions were needed in the reconstitution of proteoliposomes for each ion system. In the case of protons, a procedure reported elsewhere was followed (5). Some minor modifications in the preparation of the related buffer solutions were required for the sodium and lithium ions. The details of the purification of CF_0F_1 and the preparation of proteoliposomes are described in the Supporting Material.

The rates of ATP synthesis catalyzed by CF_0F_1 were measured at 23°C. Proteoliposomes were energized by an acid-base transition and/or lithium or sodium concentration gradients. If a membrane potential was needed, the potassium/valinomycin diffusion potential was applied across the liposome membrane. The ATP concentration was monitored continuously, using the luciferin/luciferase ATP bioluminescence assay method. Details of measurement procedures are described in the Supporting Material.

Fig. 1 depicts a schematic diagram of the final general experimental layout of the proteoliposomes and ion concentrations of the buffer medium in a typical experimental run. These concentration notations are used throughout this report. In addition, for labeling the protomers of ATP synthases, the notations III(c) and IV(a) were adapted to accommodate the two different notation conventions for the III and IV protomers in the CF_0F_1 system, and for the homologous c and a protomers in the EF_0F_1 and Na^+-F_0F_1 systems.

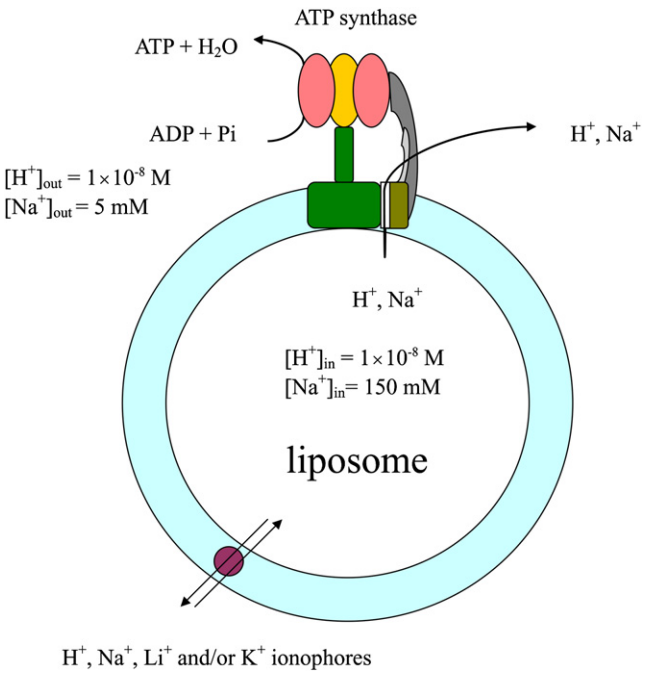

FIGURE 1 Schematic diagram of CF_0F_1 proteoliposome in experimental sample cell. An example of ionic concentrations inside and outside the proteoliposome in a specific experimental run is indicated. Notation conventions shown here were used throughout this report.

In this study, four types of ionophores were used for either the generation of a diffusion potential or simply the quenching of an ion concentration gradient in the proteoliposomes. They were: 1), the proton ionophore (carbonylcyanide-4-trifluoromethoxyphenyl hydrazone [FCCP]); 2), the potassium ionophore (valinomycin); 3), the sodium ionophore (*N*,*N*′-dibenzyl-*N*,*N*′-diphenyl-1,2-phenylenedioxydiacetamide); and 4), the lithium ionophore (6,6-dibenzyl-1,4, 8,11-tetraoxacyclotetradecane).

Measurements of the deuterium isotope's effects on the activities of CF_0F_1

The deuterium isotope's effects on the initial rates of ATP synthesis of the reconstituted ATP synthase were measured. Because it was not practical in these experiments to prepare a 100% D_2O reconstituted ATP synthase system, a series of D_2O enrichment systems with D_2O mole fractions in a range of 0–95% were prepared. The D_2O contents of the final reconstituted proteoliposomes were determined by gas chromatography/mass spectrometry. The external deuterated buffer solutions were then prepared according to the D_2O contents of the proteoliposome solutions used. The ATP synthesis rates were measured in the usual way. Here, the final effects of isotopes in the pure D_2O systems involved the extrapolated values from these measurements. The acidities of H_2O/D_2O solutions are denoted as pL instead of the normal pH notation. The details of experimental procedures for the measurement of the deuterium isotope's effects are given in the Supporting Material.

Ab initio molecular orbital calculations

The lithium and sodium ions inside the CF_0 ion channel are expected to be solvated by the side chains of the amino-acid residues of Glu, Asp, Asn, and Gln, and by some additional water molecules carried along with them. The possible chemical transformations within the solvated lithium and sodium ions were calculated by the polarizable continuum (PCM) model implemented in the Gaussian package (16). The geometric structures and energetics of solvated lithium and sodium ions were calculated according to ab initio molecular orbital methods. The deuterium isotope's effects on the equilibrium constants of chemical reactions involved in the possible proton translocation of CF_0F_1 induced by lithium or sodium ions in ion channels were also calculated. The details of these calculations are provided in the Supporting Material.

RESULTS AND DISCUSSION

Enzyme activities of CF_0F_1

As mentioned previously, the enzyme activities of CF_0F_1 from spinach were well-characterized by Gräber et al. (3–7,14). Two series of ATP synthesis-rate measurements were first performed to check the activities of CF_0F_1 against those reported in the literature: 1), at $\Delta\varphi(K^+) = 0$, the variation of the initial ATP synthesis rates as the ΔpH value varied from 1–4.8; and 2), at a fixed ΔpH value, the variation of synthesis rates as the $\Delta\varphi(K^+)$ potential varied from 0–140 mV. The observed activity behaviors of the enzyme were all in good agreement with those reported by Fischer and Gräber (5). Some specific measurements were detailed as follows. At $\Delta pH = 4.8$ ($pH_{out} = 8.8$, $pH_{in} = 4.0$) and $\Delta\varphi(K^+) = 0$ mV ($[K^+]_{in} = [K^+]_{out} = 130$ mM), the initial synthesis rate was measured as 207 s^{-1}. This value was consistent with the reported value of 190 s^{-1} measured under

conditions of $\Delta pH = 4.1$ ($pH_{out} = 8.8$, $pH_{in} = 4.7$) and also $\Delta\varphi(K^+) = 0$ mV ($[K^+]_{in} = [K^+]_{out} = 130$ mM) (5). For CF_0F_1, the initial synthesis rates gradually approached a plateau value of ~200 s^{-1} when the ΔpH values were higher than ~4.2. In another case, with a ΔpH value of 3.6 ($pH_{out} = 8.8$, $pH_{in} = 5.2$) and $\Delta\varphi(K^+) = 140$ mV ($[K^+]_{in} = 0.5$ mM, $[K^+]_{out} = 120$ mM), the synthesis rate was measured as ~200 s^{-1}. This value was in good agreement with the reported rate of 230 s^{-1} measured under the same experimental conditions (5). A typical experimental measurement is shown in Fig. S1 in the Supporting Material. These preliminary measurements ensured that the present CF_0F_1 systems functioned in the same manner as those reported in the literature.

Finally, CF_0F_1 is a complicated and delicate system, and the purification of CF_0F_1 is a lengthy operation. There were always variations in the measured ATP synthesis rates over different batches of purified CF_0F_1 that were prepared from different spinach crops. These included crops that had been planted during different growing seasons. It was not possible to attribute these variations solely to the spinach itself or to the preparation procedure of CF_0F_1. It appeared that both factors contributed to the variations. Only CF_0F_1 with synthesis rates within 15% of the reported normal values were used in our experiments. With the same batch of purified CF_0F_1 and under the same experimental conditions, the percent standard deviation of the measurements was normally within 4%. In this study, the same batch of purified CF_0F_1 was always used for measurements in which comparisons among experimental data were required. If not otherwise specified, the standard percent errors of our measurements were taken to be 4%.

Concentration gradient effects of sodium ions on the activities of CF_0F_1

The sodium ion can act as a chemical potential carrier to drive the ATP synthesis reactions of CF_0F_1

Fig. 2 shows the ATP synthesis yields driven by sodium ions under various experimental conditions. With a sodium concentration gradient of $[Na^+]_{in}/[Na^+]_{out}$ =150 mM/8 mM and $\Delta pH = 0$ ($pH_{in} = pH_{out} = 8.0$), an initial rate of 3.5 s^{-1} was evident, as shown in Fig. 2 (*curve a*). To confirm that the measured ATP molecules were not generated through any residual ΔpH, the proton gradient of the proteoliposomes (if it existed at all) was quenched by the addition of 20 μM proton ionophore FCCP. The observed ATP signal remained the same as before (Fig. 2, *curve b*). However, if 30 μM of sodium ionophore were added instead, the original ATP synthesis reactions were no longer detectable (Fig. 2, *curve c*). On the other hand, if a membrane potential of 30 mV was applied to the original sodium proteoliposome system by adding 40 μM valinomycin, the initial ATP synthesis rate increased from 3.5 to 14.7 s^{-1} (Fig. 2, *curve d*). To further confirm the origin of the observed ATP synthesis reaction in Fig. 2 (*curve d*), both

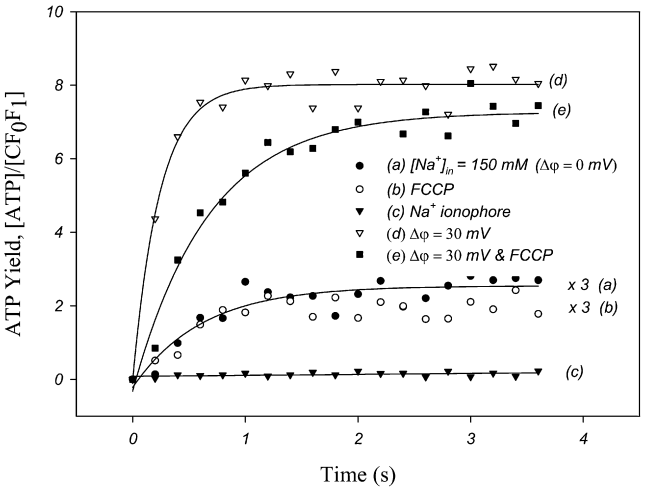

FIGURE 2 Effects of sodium ions inside proteoliposomes on ATP synthesis activities of CF_0F_1. In five experiments, concentrations of $[Na^+]_{in}/[Na^+]_{out} = 150$ mM/8 mM, and $pH_{in} = pH_{put} = 8.0$, remained the same. Curve *a*, ATP yield with $\Delta\varphi = 0$ mV. The fitted initial rate is 3.5 s^{-1}. Curve *b*, adding proton ionophore FCCP. Curve *c*, adding sodium ionophore. Curve *d*, applying a potassium membrane potential of 30 mV ($[K^+]_{out}/[K^+]_{in}$= 130 mM/50 mM). The fitted initial rate is 14.7 s^{-1}. Curve *e*, under conditions of curve *d*, plus addition of FCCP. The fitted initial rate is 9.5 s^{-1}. Each signal trace represents a single experimental measurement of ATP concentration.

FCCP and valinomycin were added to the proteoliposomes simultaneously, and the initial rate decreased from 14.7 to 9.5 s^{-1} (Fig. 2, *curve e*). The last two measurements suggest that the membrane potential could enhance Na^+ ions in driving ATP synthesis reactions ($V_i = 9.5$ s^{-1}, $\Delta\varphi = 30$ mV), and the drop of 5.2 s^{-1} from 14.7 s^{-1} to 9.5 s^{-1} could be attributed to the contribution of protons. Under the present experimental conditions of $\Delta\varphi = 30$ mV, $\Delta pH = 0.0$ ($pH_{in} = pH_{out} = 8.0$), and in the absence of sodium ions, ATP synthesis reactions were not detectable. The phenomenon of sodium ions inducing ATP synthesis reactions through the generation of protons in CF_0F_1 was also observed in the lithium ion systems. We will give a detailed account of this specific behavior of alkali metal ions below, when dealing with the effects of lithium ion concentration on enzyme activities.

In the above experiments, although the working ranges of both the concentration gradients and the membrane potentials were restricted by electrolyte concentration requirements in maintaining the stability of proteoliposomes, the experimental observations suggest that the sodium ion could act as a chemical potential carrier in driving ATP synthesis reactions in CF_0F_1. Nevertheless, the synthesis rates were only about one tenth of those of the protons. Because the concentration of protons in these experiments was on the order of 10^{-5} M, whereas that of sodium ions was 10^{-1} M in the proteoliposome systems, one could estimate, taking the above relative synthesis rate into account, that the proton is ~10^5 more efficient than the sodium ion in energizing ATP synthesis reactions in CF_0F_1.

It is interesting to compare these results with those of Na^+-F_0F_1. The ATP synthesis rates of Na^+-F_0F_1 were reported to be on the order of 1 s^{-1} for *P. modestum* (10), and 50–70 s^{-1} for *I. tartaricus*, under different experimental conditions and measurement methods (11). The latter values were accepted as normal for the Na^+-F_0F_1 systems (13). Comparing these rates of Na^+-F_0F_1 with those obtained in CF_0F_1, the activity of CF_0F_1 driven by sodium ions is one order of magnitude less efficient than that of Na^+-F_0F_1.

Concentration gradient effects of sodium ions on the activities of CF_0F_1 that are simultaneously driven by a proton gradient

In a proteoliposome, a higher sodium ion concentration can be present on either side of the membrane. To begin with, we considered that higher sodium ion and proton concentrations were present simultaneously on the inner side of the liposome. Fig. 3 shows the variation in relative initial synthesis rates as a function of $\log([Na^+]_{in}/[Na^+]_{out})$ under conditions of $[Na^+]_{out} = 1$ mM and $\Delta pH = 3.5$. Because it was shown that sodium ions are about an order of magnitude less efficient than protons in driving the ATP synthesis reaction, the initial decrease of synthesis rates shown in Fig. 3 is expected. However, the pronounced increase in synthesis rate as sodium ion concentrations are raised toward 100 mM suggests that both protons and sodium ions are simultaneously taking part in the reaction. It was established by Turina et al. (6) and Steigmiller et al. (7) that a translocation of four protons is required for each ATP molecule being synthesized in CF_0F_1. In this case, it was expected that $CF_0(H^+)_4$, $CF_0(H^+)_3(Na^+)$, $CF_0(H^+)_2(Na^+)_2$, …, etc., could sequentially contribute their shares in the ATP synthesis reaction as the sodium ion concentration increased. By adapting the functional form of Eq. (4) in this study, as will be discussed below in the context of dealing with the blocking effects of lithium ions on ATP synthesis rates, the functional forms of the relative reaction rates for the above possible CF_0 states could be represented as $1/\{1+(a[Na^+])^4\}$, $c[Na^+]/\{1+(b[Na^+])^3\}$, $(e[Na^+])^2/\{1+(d[Na^+])^2\}$, …, etc., where both the proton gradient and $[Na^+]_{out}$ are kept constant. Here a, b, c, …, etc., are parameters to be determined by experiments. We found that the experimental relative synthesis rates R shown in Fig. 3 could be adequately fitted by the functional form consisting of the first and third terms mentioned above:

$$R([Na^+]) = \frac{1}{1 + (a[Na^+])^4} + \frac{(e[Na^+])^2}{1 + (d[Na^+])^2}. \quad (1)$$

The result is shown as the smooth curve in Fig. 3. The other possible functional forms, such as the exponent 4 of the denominator of the first term being replaced by 3 or 5, or the exponent 2 of the numerator of the second term being replaced by 1 or 3, could not describe the experimental data in a similarly satisfactory way. The contribution of the linear $[Na^+]$ term was negligible. These results indicate that under the present experimental conditions, both $CF_0(H^+)_4$ and $CF_0(H^+)_2(Na^+)_2$ contribute to ATP synthesis rates, and the efficiency of ATP synthesis by the latter two-proton/two-sodium ion channel is comparable to the original four-proton ion channel. Similar competitive behavior was also observed at $\Delta pH = 4.0$. In short, this study suggests that sodium ions can compete with protons to occupy the same binding site in the CF_0 subunit during the ATP synthesis reaction. Nevertheless, to understand the underlying molecular mechanism for the cooperative behavior between sodium ions in this ATP synthesis reaction, further studies are needed.

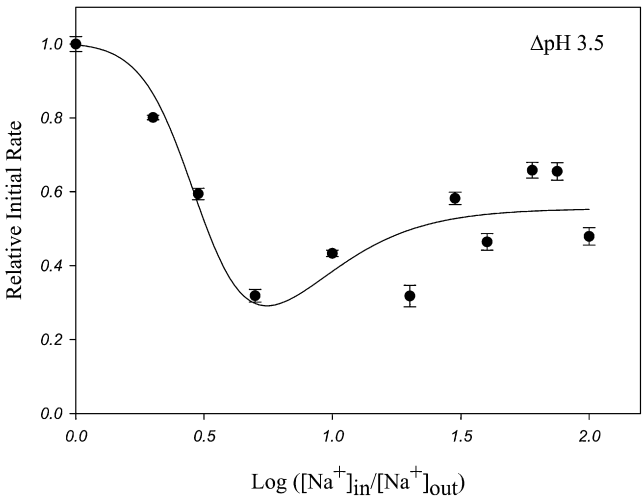

FIGURE 3 Competition of Na^+ inside proteoliposome on driving ATP synthesis reaction under conditions of $\Delta pH = 3.5$ ($pH_{out}/pH_{in} = 8.8/5.3$), $[Na^+]_{out} = 1$mM, and $[Na^+]_{in}$ at a range of 1–100 mM. Smooth curve represents simulation with Eq. (1), where $a = 0.341 \pm 0.035$, $d = 0.146 \pm 0.051$, and $e = 0.108 \pm 0.032$ mM^{-1}. Each experimental data point represents the result of two independent experimental measurements. The same batch of CF_0F_1 sample was used throughout the experiments.

Closely related enzyme behaviors were also observed in the Na^+-F_0F_1 system by Dimroth (8) and Neumann et al. (9). They concluded that sodium ions and protons on the same internal side of proteoliposome may compete for a common binding site within the F_0 sector of *P. modestum* and *I. tartaricus*, and that the mechanism for the translocation of these different ions may be the same (8,9). Apparently, these conclusions are equally applicable to the present CF_0F_1 system.

Next we considered the case where external proteoliposomes had higher sodium concentrations. At either $\Delta pH = 4.0$ or $\Delta pH = 3.3$, the initial synthesis rates were virtually unchanged as the external sodium ion concentrations were varied over the range of $[Na^+]_{in}/[Na^+]_{out} = 2$ mM/(2–300 mM). It is interesting that at $\Delta pH = 4.0$ and $[Na^+]_{in}/[Na^+]_{out} = 2$ mM/300 mM, the initial synthesis rate of CF_0F_1 would increase from 188 s^{-1} to 274 s^{-1} upon the addition of the sodium ionophore. Evidently a sodium diffusion potential ($\Delta\varphi$, ~130 mV) was generated and acted like the usual potassium diffusion potentials. These observations suggest that the external sodium ions did not affect the normal ATP synthesis process

in CF_0F_1. In contrast, for the Na^+-F_0F_1 system, it was observed that external sodium ions could bind to specific sites of F_0 and inhibit the proton translocation process (8).

In summary, the effects of sodium ions on the activities of CF_0F_1 were asymmetric with respect to their presence either inside or outside the proteoliposomes. The sodium ions that were present inside the proteoliposomes could compete with protons for the common biding site in CF_0F_1 during the normal ATP synthesis reaction, whereas those sodium ions outside the proteoliposomes showed no effects on the normal enzyme activity driven by a proton gradient. The lack of any effect on normal ATP synthesis reactions for external sodium ions indicated that the internally exposed cation-binding sites of CF_0 are not readily accessible from outside the proteoliposome.

Concentration gradient effects of lithium ions on activities of CF_0F_1

The lithium ion itself is not a chemical potential carrier in the ATP synthesis of CF_oF_1

However, in the presence of lithium ions, ATP synthesis reactions could proceed noticeably if the enzymes were driven by a membrane potential. Fig. 4 shows the experimental measurements on the effects of lithium ions in the activities of ATP synthesis under various conditions. The experimental conditions were similar to those of sodium ions, with the replacement of sodium ions by lithium ions. At $[Li^+]_{in}/[Li^+]_{out}$ = 150 mM/8 mM and $pH_{in} = pH_{out}$ = 8.0, as shown in Fig. 4 (*curve a*), no synthesis signals were detected. However, with the application of a membrane potential of 140 mV, the initial synthesis rate increased to 13.2 s^{-1} (Fig. 4, *curve b*). Decreasing the lithium ion concentration to $[Li^+]_{in}/[Li^+]_{out}$ = 10 mM/5 mM, we obtained a lower synthesis rate of 8.4 s^{-1} (Fig. 4, *curve c*). All these ATP synthesis signals were quenched completely when 10 μM proton ionophore FCCP was introduced simultaneously with the potassium ionophore to the reaction system (Fig. 4, *curve d*). At $\Delta pH = 0$ ($pH_{in} = pH_{out} = 8.0$) and $\Delta\varphi$ (K^+) = 140 mV, and in the absence of lithium ions, ATP synthesis reactions were not detectable in this experiment. Furthermore, at $\Delta\varphi(K^+)$ = 140 mV and $\Delta pH = 0$, the synthesis rate measured under conditions of $[Li^+]_{in}/[Li^+]_{out}$ = 75 mM/5 mM was essentially identical to that at $[Li^+]_{in}/[Li^+]_{out}$ = 75 mM/75 mM. In other words, under the above experimental conditions, the external lithium ions did not affect ATP synthesis rates. These measurements indicate that the role of lithium ions in the activities of CF_0F_1 is different from that of sodium ions. In the presence of lithium ions, the ATP synthesis reaction was actually driven by the translocation of protons through CF_0, and the lithium ions were only indirectly involved in this process. Below, we present further experimental and theoretical studies to support this proposition.

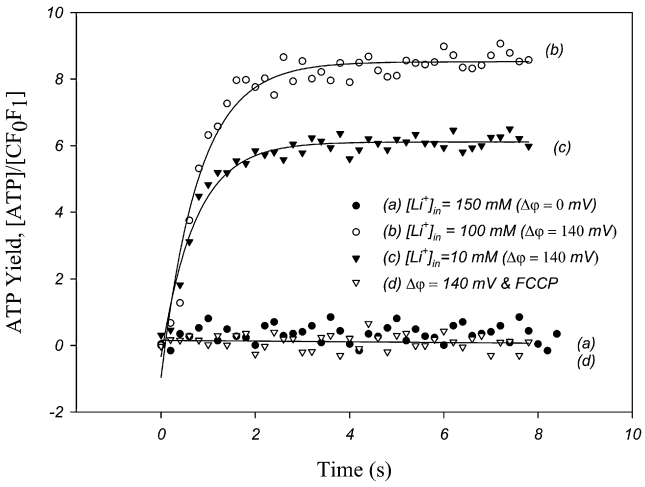

FIGURE 4 Effects of lithium ions inside proteoliposomes on ATP synthesis activites of CF_0F_1. Curve *a*, ATP yield with $[Li^+]_{in}/[Li^+]_{out}$ =150 mM/5 mM and $\Delta\varphi = 0$ mV. Curve *b*, $[Li^+]_{in}/[Li^+]_{out}$ = 100 mM/5 mM and $\Delta\varphi$ = 140 mV. The fitted initial rate is 13.2 s^{-1}. Curve *c*, $[Li^+]_{in}/[Li^+]_{out}$ = 10 mM/5 mM and $\Delta\varphi$ =140 mV. The initial rate is 8.4 s^{-1}. Curve *d*, under conditions of curve *b*, plus addition of FCCP. Each signal trace represents a single experimental measurement of ATP concentration.

In an adequate molecular environment, lithium ions can generate a local proton concentration through localized hydrolysis reaction

In studying the activity coefficients of alkali metal salts in aqueous solutions, Robinson and Harned (17) and Harned and Owen (18) suggested that lithium and sodium ions have a greater tendency to undergo localized hydrolysis by reacting with anions with a good proton-accepting capability. The net reaction may be represented by

$$M^+ + H_2O + A^- \rightleftarrows M^+ \cdots OH^- \cdots H^+ \cdots A^- \quad (2)$$

in which M^+ is the alkali metal ion, A^- is a proton acceptor such as a hydroxide or acetate anion, and the dotted lines represent linkages attributable to ion-solvent molecule forces. Here, depending on the local chemical environment of alkali metal ions, the solvent molecules could be any nonreactive organic or inorganic compound. Equation (2) implies that the original free ions on the reactant side become a loosely bound complex through the local hydrolysis reaction. In other words, the alkali metal ions carry a certain amount of proton, as well as hydroxide ion, atmosphere around them. Among the alkali metal ions, it was suggested that lithium and sodium ions have the greatest tendency to undergo a localized hydrolysis reaction (17,18). Although the concept of localized hydrolysis was proposed to rationalize the abnormality of the activity coefficients of, say, aqueous lithium hydroxide, a direct observation of the enhancement of the local proton or hydroxide ion concentration around the alkali metal ion has not been amenable to

experiments for some time. It appears that under appropriate local molecular arrangements, e.g., in the ion channel of CF_0F_1, this specific proton-generation property could manifest itself in the ion translocation process, and could be tested.

Based on the concept of localized hydrolysis reactions and the experimental information obtained here, the equivalent proton concentration in the ion channel could be estimated as follows. At $\Delta\varphi = 140$ mV, the ATP synthesis rate with 100 mM of Li^+ is equal to that with $\Delta pH = 1.7$ without the involvement of the lithium ions. This means that, in the presence of 100 mM Li^+ and at $pH_{out} = 8.0$, the equivalent proton concentration in the ion channel is on the order of pH_{in} ~6.3 ($[H^+]_{in}$, ~5×10^{-7} M). In the following discussion of ab initio molecular orbital calculations, we shall give a detailed theoretical account of the localized hydrolysis reaction by considering the probable local ion structures and corresponding local proton concentrations in the specific chemical environment of the CF_0 ion channel. Before proceeding to this subject, we shall complete the experimental studies on the deuterium isotope's effects and the blocking behaviors of lithium ions on the activities of CF_0F_1.

Deuterium isotope effects on CF_0F_1 activities originating in the lithium ions

To identify the possible active species involved in the ATP synthesis reactions of CF_0F_1 in the presence of lithium ions, the deuterium isotope's effects on ATP synthesis rates were measured. To extract the deuterium isotope's effects that originated purely in the lithium ions, the deuterium isotope's effects on the native CF_0F_1 and on CF_0F_1 under similar experimental conditions but in the presence of lithium ions were measured.

Under conditions of $\Delta\varphi = 0$ and $pL_{out} = 8.8$, the deuterium isotope's effects on ATP synthesis rates, $V_i(D_2O)/V_i(H_2O)$, were measured as 0.67 ± 0.05 and 0.66 ± 0.05 at two different proton gradients of $\Delta pL = 4.0$ and 3.5, respectively. This suggests that without the membrane potential, the deuterium isotope's effects on synthesis rates were insensitive to the above differences in proton gradients. However, in the presence of a membrane potential, the extent of the isotope's effects varied with the ΔpL value. Fig. 5, *a* and *b*, shows that at $\Delta\varphi = 140$ mV and $pL_{out} = 8.0$, the isotope's effects were measured as 0.33 ± 0.09 and 0.58 ± 0.06, with $\Delta pL = 3.0$ and 1.7, respectively. Here it was found that in pure H_2O and at $\Delta\varphi = 140$ mV, the synthesis rate obtained under conditions of $\Delta pH = 1.7$ ($pH_{out} = 8.0$) and $[Li^+]_{in} = 0.0$ mM was identical to that with $[Li^+]_{in} =$ 100 mM and $\Delta pH = 0$ ($pH_{out} = 8.0$). The deuterium isotope's effect under the latter conditions was then measured as 0.27 ± 0.09, as shown in Fig. 5 *c*. By taking the ratio of the measured isotope effects obtained in Fig. 5, *b* and *c*, the deuterium isotope's effect because of the presence of lithium ions was determined to be 0.27/0.58 = 0.46(±0.16). In this calculation, it was assumed that the variation of the experimental pH_{in} value from 6.3 to 8.0 did not affect the deuterium isotope's effects on the systems. In support of this assumption, the deuterium isotope's effects on proton conductance through the CF_0 subunit of the pea chloroplasts were measured as 0.58, and the measured conductance isotope's effects were found to be pL-independent over a range of 5.6–8.0 (19,20).

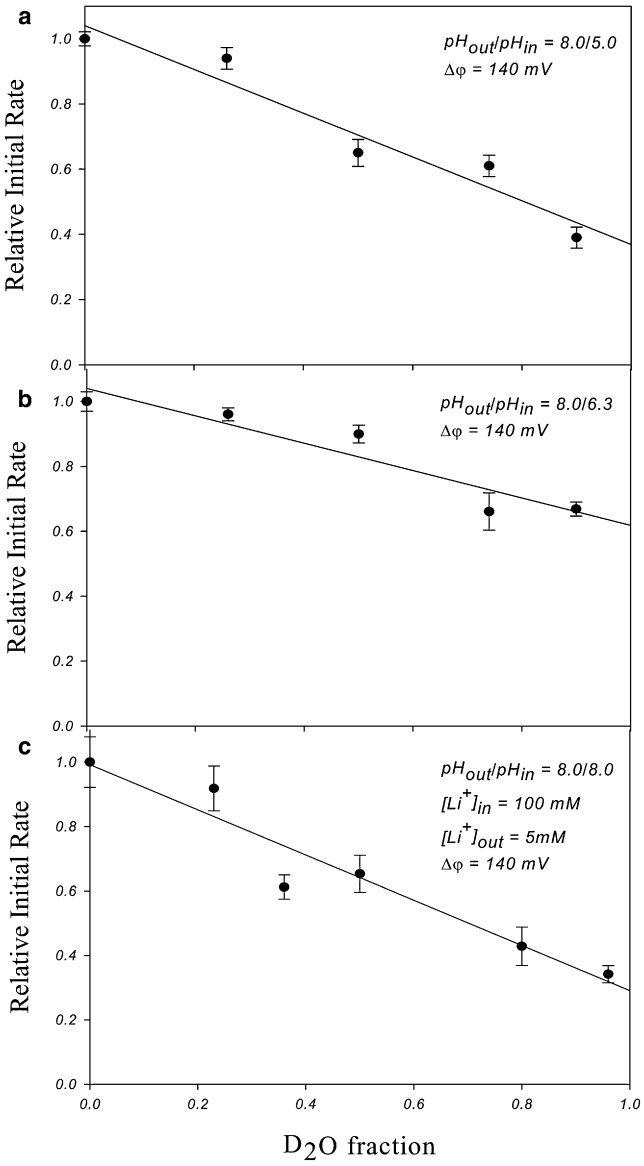

FIGURE 5 Deuterium isotope's effects on relative initial ATP synthesis rates of CF_0F_1. Membrane potentials were all set at 140 mV. Experimental conditions are: (*a*) $pH_{out}/pH_{in} = 8.0/5.0$, (*b*) $pH_{out}/pH_{in} = 8.0/6.3$, and (*c*) $pH_{out}/pH_{in} = 8.0/8.0$, and $[Li^+]_{in}/[Li^+]_{out}$ =100 mM/5 mM. Each experimental data point represents the result of four independent experimental measurements. The same batch of CF_0F_1 sample was used throughout the experiments.

To see the implications of these measured deuterium isotope effects, we refer to the current understanding of the deuterium isotope's effects on the ion conductance of sodium, potassium, and proton ion channels in cells. These ion channels are selective in specific ions for permeation,

and their deuterium isotope effects were well-studied (21–23). For sodium-specific and potassium-specific ion channels, expressed as a ratio of D_2O/H_2O, the deuterium isotope's reported effects fell roughly in the range of 0.83–0.68 (21,22). In these systems, it was rationalized that the deuterium isotope's effects on ion conductance were mainly attributable to differences in viscosity, mobility, or the mass of the inner-shell solvated ions between the D_2O and H_2O systems. These measured values simply reflect that for these sodium and potassium ion channels, protons were not directly involved in the rate-limiting step of the ion permeation process. In contrast, for proton ion channels, the deuterium isotope's effects on proton conductance were measured as 0.53, a more pronounced value than those in the cases of sodium and potassium (23). It was suggested that the protons were interacting specifically with the channel, and simultaneously carrying the current during permeation (23). Following the same line of argument, for the CF_0F_1 enzyme, the pronounced effects of the deuterium isotope originating in the lithium ions indicated that protons were the active species involved in the translocation process in CF_0 ion channels. The two other most plausible ion candidates (lithium ions and hydroxide ions) were ruled out in terms of participating directly in carrying the ion current during ATP synthesis reactions.

It is interesting that the reported deuterium isotope's effects on proton conductance through CF_0 of pea chloroplasts in the near-neutral pH regime (19) were identical to those on the CF_0F_1 activities operated at a membrane potential and in a similar pH range, as shown in Fig. 5 *b*. Because the isotope's effects on ATP synthesis rates could be regarded as a net result of both proton translocation in CF_0 and the synthesis reaction of ATP from ADP and the phosphate ion by CF_1, these results suggest that the deuterium isotope's effects on the latter process are negligible.

Blocking effects of lithium ions inside proteoliposomes on the activities of CF_0F_1

The effects of internal lithium ions on ATP synthesis rates were measured at $\Delta pH = 4.4$ and 3.5. At $\Delta pH = 4.4$ ($pH_{out} = 8.8$, $pH_{in} = 4.4$) and under lithium ion concentrations of $[Li^+]_{in}/[Li^+]_{out} = 1$ mM/1 mM and $[Li^+]_{in}/[Li^+]_{out} = 100$ mM/1 mM, respectively, our experiments showed that lithium ions inside the proteoliposome essentially exerted no inhibitive effects on enzyme activities. The measurements are shown in Fig. S2. However, at $\Delta pH = 3.5$, synthesis rates were drastically reduced by higher lithium ion concentrations. Fig. 6 shows the measured relative initial rates as the lithium ion concentration was varied from 1 mM to 75 mM. In Fig. 6, the synthesis rates were corrected using the small but nonnegligible contribution of lithium ions through the localized hydrolysis reaction. Evidently, lithium ions can quite effectively block the normal proton translocation in CF_0F_1. To analyze this blocking behavior quantitatively, we resorted to the classical blocking model developed for the

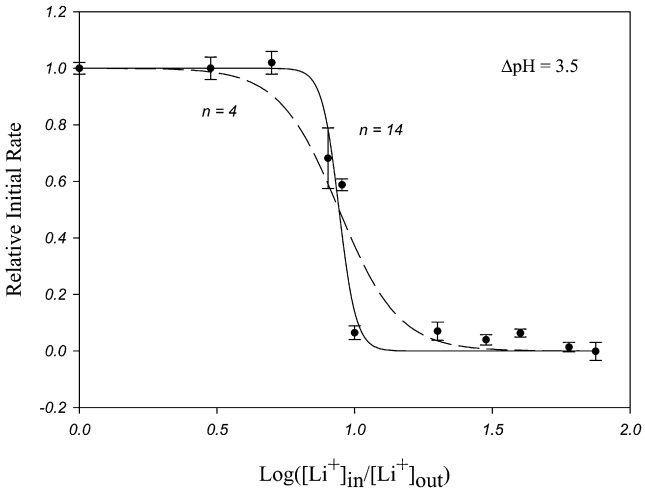

FIGURE 6 Blocking effects of Li^+ inside proteoliposome under conditions of $\Delta pH = 3.5$ ($pH_{out}/pH_{in} = 8.8/5.3$), $[Li^+]_{out} = 1$ mM, and $[Li^+]_{in}$ at a range of 1–75 mM. Two fitted curves were results of Hill coefficient n set at 4 and 14, respectively. Original experimental data were corrected with the residual synthesis rates originating from the localized hydrolysis of lithium ions. A strong cooperative blocking effect on the ATP synthesis rate was observed. Each experimental data point represents the result of two independent experimental measurements. The same batch of CF_0F_1 sample was used throughout the experiments.

analysis of ion currents in the ion channels of excitable membranes, e.g., sodium and potassium ion channels. For these ubiquitous ion channels of excitable cells, the general blocking mechanisms and their kinetic behaviors between the ion currents of different ionic and/or neutral species have been studied extensively (24). Despite the functional differences between ion channels of excitable cells and the CF_0F_1 of chloroplasts, the lithium ion-blocking behavior on the ATP synthesis reaction in the ion channel of CF_0F_1 can be analyzed by the basic blocking model proposed by Woodhull (25) and the related Hill equation developed for conventional ion channel systems (26). The dissociation constant of Li^+ from the binding site is assumed to be in the form of:

$$K_{Li}(\varphi) = K_{Li}(0)\exp(-Z\varphi F/RT) \quad (3)$$

in which $K_{Li}(0)$ is the dissociation constant of Li^+ at zero potential, Z is the effective valency of Li^+, φ is the membrane potential, and F is the Faraday constant. The relative ATP synthesis rates as a function of blocker concentration are then fitted with the Hill equation:

$$\frac{V_i([Li^+])}{V_i(0)} = \frac{1}{1 + \left(\frac{[Li^+]}{[K_{Li}(\varphi)]}\right)^n} \quad (4)$$

in which $V_i(0)$ and $V_i([Li^+])$ are the synthesis rates with lithium ion concentrations at 0 and $[Li^+]$, respectively, and n is the Hill coefficient. Here, φ is set at 0 mV.

Fig. 6 shows the fitted curves with n being set at 4 and 14, respectively. The former value is the number of protons

needed to be translocated to synthesize one ATP molecule (3,6,7), and the latter value is the stoichiometric number of the III(c) protomer in the III(c) ring of CF_0F_1 (27). For the other n value in the range of 4–14, the corresponding curve falls between these two fitted curves. In the case of $n = 4$, the goodness of fit to the experimental data appears to be only fair. Nevertheless, the fitted curve can already capture the general blocking features of the lithium ions. If the ATP synthesis reaction of CF_0F_1 is taken to proceed in the sequence of each individual ATP synthesis step, this blocking behavior is comparable to the earlier kinetics observations of Possmayer and Gräber (3), which state that the ATP synthesis rate in CF_0F_1 is best described by a four-proton sequential-binding reaction mechanism. However, as one goes to $n = 14$, the fitted curve can quite adequately represent the experimental data. Although the other neighboring n values appear to be equally appropriate in describing the experimental data, the results presented here strongly suggest that the blocking of ATP synthesis by lithium ions occurs through a cooperative inhibition of the whole CF_0F_1 activity instead of the sequential proton ion blocking in each individual ATP synthesis step. In one respect, this implies that in the course of the reaction, all 14 ion-binding sites of the III(c) ring were occupied by lithium ions. However, this seemingly improbable blocking behavior could be achieved by simply blocking the entrance ion channel of CF_0 by one lithium ion. We shall discuss and resolve this issue by examining the local protein structures of the ion channel in CF_0 in our final theoretical discussion.

Blocking effects of lithium ions outside proteoliposomes on activities of CF_0F_1

The effects of external lithium ions on enzyme activities were studied at $\Delta pH = 4.0$ and 3.3. At $\Delta pH = 4.0$ and $[Li^+]_{in} = 3.0$ mM, ATP synthesis rates remained essentially unchanged as the external lithium ion concentrations varied over a range of 3–300 mM. At $\Delta pH = 3.3$, as shown in Fig. 7, the activities of CF_0F_1 were only mildly inhibited by external lithium ions. The blocking efficiency data were fitted with Eq. 4, and the fitted Hill coefficient was found to be 1.1. There was only a weak cooperativity in blocking behavior for the external lithium ions. Apparently the blocking behaviors of external lithium ions are drastically different from those of internal lithium ions. The inhibitive effects of sodium and lithium ions on proton uptake by the F_0-liposomes of Na^+-F_1F_0 from *P. modestum* were studied by Kluge and Dimroth (28). They concluded that that the cation-binding site of Na^+-F_0 was not accessible from both sides of the membrane simultaneously. Because the general blocking behaviors of our CF_0 system resemble those of Na^+-F_0, the conclusion reached for the Na^+-F_0 system is equally applicable to the CF_0 system.

When the external lithium ion concentration is higher than the internal ion concentration, the addition of the lithium ionophore to proteoliposomes would generate a diffusion potential in the same manner as in the K^+/valinomycin system. For instance, under conditions of $[Li^+]_{out}/[Li^+]_{in} = 300$ mM/3 mM and $\Delta pH = 3.5$ ($pH_{out} = 8.1$ and $pH_{in} = 4.6$), which is equivalent to a diffusion potential of 120 mV at room temperature, upon the addition of the lithium ionophore, the measured ATP synthesis rate increased from 64 s^{-1} to 205 s^{-1}. The blocking effects induced by external lithium ions on enzyme activities were literally annihilated by the diffusion potential generated through the lithium concentration gradient.

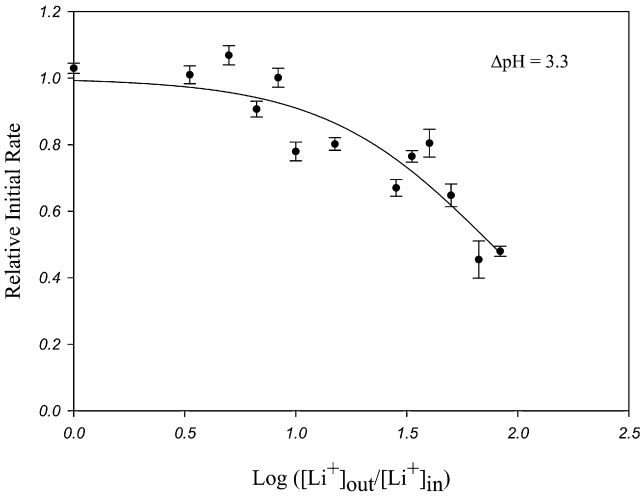

FIGURE 7 Blocking effects of Li^+ outside proteoliposome under conditions of $\Delta pH = 3.3$ ($pH_{out}/pH_{in} = 8.0/4.7$), $[Li^+]_{in} = 3$ mM, and $[Li^+]_{out}$ at a range of 3–300 mM. The fitted Hill coefficient n is 1.1. A weak cooperative blocking effect on ATP synthesis rates was observed. Each experimental data point represents the result of four independent experimental measurements. The same batch of CF_0F_1 sample was used throughout the experiments.

Ab initio molecular orbital calculations on the energetics and deuterium isotope's effects on localized hydrolysis reactions in solvated Li^+ and Na^+ systems, which are related to the ion translocation process in the ion channel of CF_0

We shall only give a brief account of the calculation procedures and final main results. Details are described in the Supporting Material. To begin with the calculations, one first needs to determine the composition of the first solvation shell of the lithium and sodium ions in the ion channel. The amino-acid residues that were reported as critical for the translocation of the ions or lining along the aqueous access ion channel in the F_0 subunits of *E. coli*, *P. modestum*, and *I. tartaricus* are well-established in the literature (12,13,29–31). The conservation of these specific amino-acid residues among the four F_0 homologs considered here indicates that the amino-acid sequences of CF_0 simultaneously possess the essential features of those of EF_0 and Na^+-F_0. With a knowledge of local protein structures of EF_0 and Na^+-F_0, and the assumption that local protein structures are conserved

among the homologs, the possible first solvation shell of the lithium and sodium ions in CF_0 can be specified. The geometric structures, energetics, and deuterium isotopes of the localized hydrolysis reactions of solvated ions were calculated using ab initio molecular orbital methods (16).

Based on the theoretical energetics of localized hydrolysis reactions, one can calculate the local enhancement of proton concentration attributable to the presence of lithium or sodium ions in the molecular environment of the ion channel of CF_0. In the case of the lithium ion, the theoretical enhancement value was equivalent to a decrease of $\Delta pH = 1.6$ in a near-neutral aqueous solution. For comparison, we found experimentally that at $[Li^+]_{in} = 100$ mM, the equivalent proton concentration was decreased by $\Delta pH = 1.7$, as manifested in the ATP synthesis rates of CF_0F_1. Considering the approximations in the above theoretical calculations, the agreement between the experimental value and the theoretical estimation of the proton concentration enhancement is very good.

Depending on the structures of the first solvation shell, the theoretical effects of the deuterium isotope on the equilibrium concentrations of lithium systems were calculated at a range of 0.24–0.72. Here, the deuterium isotope's effects were measured as 0.46, a value falling approximately within this range of theoretical values. The agreement is considered reasonably good. A rationalization of the variations between the experimental and theoretical effects of the deuterium isotope is proposed in the Supporting Material.

Molecular mechanisms of ion translocations in EF_0 and Na^+-F_0, and the implications of the Li^+ and Na^+ experimental results on the ion translocation mechanism in CF_0

As mentioned previously, the molecular mechanisms of torque generation through the proton translocation in EF_0, and of torque generation through the sodium translocation in Na^+-F_0, were studied intensively by two independent research groups (12,13). Despite differences in physical and chemical properties between proton and sodium ions, and also in some protein features between EF_0 and Na^+-F_0, the basic torque-generation principle is essentially the same between these two homologous systems (12,13). The amino-acid sequences of CF_0 simultaneously carry the essential sequence features of their homologs in both EF_0 and Na^+-F_0. Experimentally, it was also demonstrated that in ATP synthesis reactions, CF_0 could provide the pathway for both the protons and sodium ions. The evidence suggests that for CF_0, protons and sodium ions used the same ion translocation mechanism as those in the EF_0 and Na^+-F_0 systems during ATP synthesis reactions.

The high degree of cooperativity in the blocking behaviors of internal lithium ions suggested that lithium ions could block ATP synthesis reactions over the entire period of one full rotation in CF_0F_1. Because the proton translocation attributable to localized hydrolysis reactions still operates under the blocking of lithium ions, this implies that lithium ions do not enter and settle down in the III(c) ring, as do the sodium ions. Next we shall provide further support for the above rationalization by comparing solvation energies between the lithium and sodium systems in CF_0.

For the facts that the sodium ion is a less efficient energy transduction carrier in CF_0F_1 than in Na^+-F_0F_1, and that the lithium ion itself is a blocker in CF_0F_1, one may find an explanation in the slight structural differences in the III(c) ring between the CF_0 and Na^+-F_0 subunits. For the Na^+-F_0 subunit, it was shown that the sodium is stabilized by the side chains of Q32, E65, S66, and Y70 of III(c) (29). However, as shown in Fig. S3, the corresponding amino-acid residue of the CF_0 subunit, which is in alignment with S66 (Ser) of the III(c) protomer of Na^+-F_0, is A62 (Ala). Evidently, the side group of S66 (Ser) has a much better solvating capability than that of A62 (Ala). If one assumes that the local protein structure for Na^+ is the same in both species, then apparently the ions in CF_0 are not being as well-stabilized as those in Na^+-F_0. This minor structural variation could explain why Na^+-F_0F_1 is a more efficient Na^+-driven ATP synthase than is CF_0F_1 driven by the same ion. As for the different behaviors of the sodium and lithium ions in CF_0F_1, the possibility exists that, like Na^+-F_0, the ion solvating size of the local protein structure of the III(c) ring has being tuned to that of the sodium ions, and also that the energetic differences in stripping off a solvating molecule from the fully solvated ion to fit into the III(c) ring of CF_0. Note that, unlike Na^+-F_0, CF_0 lacks a solvating Ser amino-acid residue in III(c). Here, the energetics of a water molecule being dissociated from the first solvated shell of the ion were calculated as:

$$M^+E^-Q_2(H_2O) \rightarrow M^+E^-Q_2 + H_2O \quad (5)$$

$$(M = \text{Li or Na}).$$

In the medium with a dielectric constant of 10 and at 298 K (32), the enthalpy and Gibbs free energy of Eq. (5) are 50.1 and 7.3 kJ/mol for Li^+, and 45.3 and 0.2 kJ/mol for Na^+, respectively. The energetic differences between the Na^+ and Li^+ systems indicate that, in the above trapping process, Na^+ is preferred by III(c) to Li^+ by a factor of ~10. These structural and energetic factors could be used as further support for the lithium ion-blocking mechanism proposed in this study. Note that the dissociated free water molecule only served as a reference state. Only the relative energetic values were adapted in this discussion.

Finally, we need to clarify how the localized hydrolysis reactions of Li^+ or Na^+ assist the translocation of the proton through CF_0. The proton generated through localized hydrolysis is already in the form of a neutral carboxylic acid, and is ready for the translocation toward or into the III(c) ring. Through the application of ΔpH and/or $\Delta\varphi$, the local hydroxide ion can be readily neutralized by an incoming proton through the ion channel. The initial dipolar electric

field of the (Li^+)-(OH^-) ion pair now becomes a monopolar field originating solely from Li^+ or Na^+. The resulting electric field can now drive the rotation of the III(*c*) ring. The net result is the translocation of a proton, instead of the lithium or sodium ion itself. In the hydrolysis products, as shown in Fig. S5 *b*, both the proton and the alkali metal ion were in simultaneous interaction with the same carboxylate anion. For the lithium ion, because of the higher energy needed for translocation into the III(*c*) ring, as shown in Eq. (5), only the proton can undergo the second half of the translocation process. For the sodium ion, both the proton and the sodium ion are capable of completing the translocation process. This new ion translocation pathway can be regarded a hybridization of the two ion translocation pathways proposed independently for the proton-driven EF_0 and sodium-driven Na^+-F_0 systems (12,13). In summary, based on the unique features of the CF_0 protein, the specific enzyme behaviors of CF_0F_1 observed in this study could be rationalized in terms of the well-studied EF_0 and Na^+-F_0 models.

CONCLUSIONS

We studied the concentration gradient effects of Na^+ and Li^+, and the deuterium isotope's effects on the ATP synthesis activities of CF_0F_1 from chloroplasts. It was demonstrated that sodium ions could act like protons as a chemical potential carrier for CF_0F_1. In contrast, lithium ions acted as a channel blocker to the translocation of protons during the ATP synthesis process. In addition to these traditional activity behaviors, the unexpected enzyme behaviors of CF_0F_1 were evident when sodium or lithium ions were present and a membrane potential was applied in the enzyme systems. A new (to our knowledge) ion translocation process that involved the localized hydrolysis reactions of the lithium and sodium ions in the specific chemical environment of the ion channel of CF_0 was proposed. Experimental studies of the deuterium isotope's effects on lithium ions, and the results of ab initio molecular orbital calculations on the related molecular complex systems, supported the proposed molecular mechanism. The behaviors of the general activity of CF_0F_1 in the presence of sodium and lithium ions can be rationalized and understood in the framework of the general molecular mechanisms of ion translocations developed for the proton-driven EF_0F_1 and the sodium ion-driven Na^+-F_0F_1 reported in the literature (12,13).

SUPPORTING MATERIAL

Materials and methods, results and discussions, figures, a table, and references are available at http://www.biophysj.org/biophysj/supplemental/S0006-3495(09)00376-2.

J.-D. W. expresses his gratitude to Dr. S. Fischer of Universität Freiburg for her kind suggestions regarding the preparations of CF_0F_1 and proteoliposomes.

This work was supported by grants from the National Science Council, Taipei, Taiwan.

REFERENCES

1. Mitchell, P. 1961. Coupling of phosphorylation to electron and hydrogen transfer by chemi-osmotic type of mechanism. *Nature*. 191:144–148.
2. Mitchell, P. 1966. Chemiosmotic coupling in oxidative and photosynthetic phosphorylation. *Biol. Rev. Camb. Philos. Soc.* 41:445–502.
3. Possmayer, F. E., and P. Gräber. 1994. The pH_{in} and pH_{out} dependence of the rate of ATP synthesis catalyzed by the chloroplast H^+-ATPase, CF_0F_1, in proteoliposomes. *J. Biol. Chem.* 269:1896–1904.
4. Fischer, S., C. Etzold, P. Turina, G. Deckers-Hebestreit, K. Altendorf, et al. 1994. ATP synthesis catalyzed by the ATP synthase of *Escherichia coli* reconstituted into liposomes. *Eur. J. Biochem.* 225:167–172.
5. Fischer, S., and P. Gräber. 1999. Comparison of ΔpH- and $\Delta\varphi$-driven ATP synthesis catalyzed by the H(+)-ATPases from *Escherichia coli* or chloroplasts reconstituted into liposomes. *FEBS Lett.* 457:327–332.
6. Turina, P., D. Samoray, and P. Gräber. 2003. H^+/ATP ratio of proton transport-coupled ATP synthesis and hydrolysis catalyzed by CF_0F_1-liposomes. *EMBO J.* 22:418–426.
7. Steigmiller, S., P. Turina, and P. Gräber. 2008. The thermodynamic H^+/ATP ratios of the H^+-ATPsynthases from chloroplasts and *Escherichia coli*. *Proc. Natl. Acad. Sci. USA.* 105:3745–3750.
8. Dimroth, P. 1997. Primary sodium ion translocating enzymes. *Biochim. Biophys. Acta.* 1318:11–51.
9. Neumann, S., U. Matthey, G. Kaim, and P. Dimroth. 1998. Purification and properties of the F_1F_o ATPase of *Ilyobacter tartaricus*, a sodium ion pump. *J. Bacteriol.* 180:3312–3316.
10. Kaim, G., and P. Dimroth. 1998. Voltage-generated torque drives the motor of the ATP synthase. *EMBO J.* 17:5887–5895.
11. Burzik, C., G. Kaim, P. Dimroth, E. Bamberg, and K. Fendler. 2003. Charge displacements during ATP-hydorlysis and synthesis of the Na^+-transporting F_oF_1-ATPase of *Ilyobacter tartaricus*. *Biophys. J.* 85:2044–2054.
12. Aksimentiev, A., I. A. Balabin, R. H. Fillingame, and K. Schulten. 2004. Insights into the molecular mechanism of rotation in the F_0 sector of ATP synthase. *Biophys. J.* 86:1332–1344.
13. Xing, J., H. Wang, C. V. Ballmoos, P. Dimroth, and G. Oster. 2004. Torque generation by the F_0 motor of the sodium ATPase. *Biophys. J.* 87:2148–2163.
14. Grotjohann, I., and P. Gräber. 2002. The H^+-ATPase from chloroplasts: effect of different reconstitution procedures on ATP synthesis activity and on phosphate dependence of ATP synthesis. *Biochim. Biophys. Acta.* 1556:208–216.
15. Rigaud, J. L., B. Pitard, and D. Levy. 1995. Reconstitution of membrane proteins into liposomes: application to energy-transducing membrane proteins. *Biochim. Biophys. Acta.* 1231:223–246.
16. Frisch, M. J., G. W. Trucks, H. B. Schlegel, G. E. Scuseria, M. A. Robb, et al. 2004. Gaussian 03, Revision C.02. Gaussian, Inc., Wallingford, CT.
17. Robinson, R. A., and H. S. Harned. 1941. Some aspects of the thermodynamics of strong electrolytes from electromotoric force and vapor pressure measurements. *Chem. Rev.* 28:419–476.
18. Harned, H. S., and B. B. Owen. 1958. The Physical Chemistry of Electrolytic Solutions, 3rd ed. Reinhold Publishing, New York.
19. Althoff, G., H. Lill, and W. Junge. 1989. Proton channel of the chloroplast ATP synthase, CF_0: its time-averaged single-channel conductance as function of pH, temperature, isotopic and ionic medium composition. *J. Membr. Biol.* 108:263–271.
20. Feniouk, B. A., M. A. Kozlova, D. A. Knorre, D. A. Cherepanov, A. Y. Mulkidjanian, et al. 2004. The proton-driven rotor of ATP synthase: ohmic conductance (10 fS), and absence of voltage gating. *Biophys. J.* 86:4094–4109.
21. Schauf, C. L., and J. O. Bullock. 1980. Solvent substitution as a probe of channel gating in *Myxicola*: differential effects of D_2O on some components of membrane conductance. *Biophys. J.* 30:295–305.

22. Schauf, C. L., and J. O. Bullock. 1982. Solvent substitution as a probe of channel gating in *Myxicola*: effects of D_2O on kinetic properties of drugs that occlude channels. *Biophys. J.* 37:441–452.

23. DeCoursey, T. E., and V. V. Cherny. 1997. Deuterium isotope effects on permeation and gating of proton channels in rat alveolar epithelium. *J. Gen. Physiol.* 109:415–434.

24. Hille, B. 2001. Ion Channels of Excitable Membranes, 3rd ed. Sinauer Associates, Sunderland, MA.

25. Woodhull, A. M. 1973. Ionic blockage of sodium channels in nerve. *J. Gen. Physiol.* 61:687–708.

26. Lopatin, A. N., and C. G. Nichols. 1994. Internal Na^+ and Mg^{2+} blockade of DRK1 (Kv2.1) potassium channels expressed in *Xenopus oocytes*, inward rectification of a delay rectifier. *J. Gen. Physiol.* 103:203–216.

27. Seelert, H., N. A. Dencher, and D. J. Muller. 2003. Fourteen protomers compose the oligomer III of the proton-rotor in spinach chloroplast ATP synthase. *J. Mol. Biol.* 333:337–344.

28. Kluge, C., and P. Dimroth. 1992. Studies on Na^+ and H^+ translocation through the F_0 part of the Na^+-translocating F_1F_0 ATPase from *Propionigenium modestum*: discovery of a membrane potential dependent step. *Biochemistry.* 31:12665–12672.

29. Meier, T., P. Polzer, K. Diederichs, W. Welte, and P. Dimroth. 2005. Structure of the rotor ring of F-type Na^+-ATPase from *Ilyobacter tartaricus*. *Science*. 308:659–662.

30. Angevine, C. M., and R. H. Fillingame. 2003. Aqueous access channels in subunit *a* of rotary ATP synthase. *J. Biol. Chem.* 278: 6066–6074.

31. Moore, K. J., C. M. Angevine, O. D. Vincent, B. E. Schwem, and R. H. Fillingame. 2008. The cytoplasmic loops of subunit *a* of *Escherichia coli* ATP synthase may participate in the proton translocating mechanism. *J. Biol. Chem.* 283:13044–13052.

32. Elston, T., H. Wang, and G. Oster. 1998. Energy transduction in ATP synthase. *Nature*. 391:510–513.